# Multimodal Gaussian Mixture Model for Realtime Roadside LiDAR Object Detection

Tianya Zhang, Ph.D., Peter J. Jin, Ph.D., Yi Ge

Abstract— Background modeling is widely used for intelligent surveillance systems to detect the moving targets by subtracting the static background components. Most roadside LiDAR object detection methods filter out foreground points by comparing new points to pre-trained background references based on descriptive statistics over many frames (e.g., voxel density, slopes, maximum distance). These solutions are not efficient under heavy traffic, and parameter values are hard to transfer from one scenario to another. In early studies, the video-based background modeling methods were considered not suitable for roadside LiDAR surveillance systems due to the sparse and unstructured point clouds data. In this paper, the raw LiDAR data were transformed into a multi-dimensional tensor structure based on the elevation and azimuth value of each LiDAR point. With this high-order data representation, we break the barrier to allow the efficient Gaussian Mixture Model (GMM) method for roadside LiDAR background modeling. The probabilistic GMM is built with superior agility and real-time capability. The proposed Method was compared against two state-of-the-art roadside LiDAR background models and evaluated based on point level, object level, and path level, demonstrating better robustness under heavy traffic and challenging weather. This multimodal GMM method is capable of handling dynamic backgrounds with noisy measurements and substantially enhances the infrastructurebased LiDAR object detection, whereby various 3D modeling for smart city applications could be created.

Index Terms — Roadside LiDAR, Background Modeling, Object Detection

# I. INTRODUCTION

LiDAR (Light Detection and Ranging) has great potential to be a beneficial element in future roadside sensor networks. For intersection analytics, wherein the majority of crashes happen, one single LiDAR device could cover an entire intersection area with accurate 3D distance measurement. While it usually needs to have multiple cameras/radars to cover one intersection from different angles. The LiDAR solution does not incur privacy concerns; therefore, it is suitable for privacy-sensitive applications, such as crowd management and people counting. LiDAR sensor could function in various environments, unlike the camera sensor, which relies on

This work is funded by the New Jersey DOT Real-time signal performance measures (Project No. 2016-14); New Brunswick Innovation Hub Smart Mobility Testing Ground (SMTG) Contract Numbers: 21-60168.

T. Zhang is a final year PhD student, and incoming Postdoc at Rutgers University, NJ 08854 USA (e-mail: tz140@soe.rutgers.edu).

external illuminations. The data collected through LiDAR could be used to optimize signal control and reduce delay and emission, as well as crowd management for event planning. Combined with the Vehicle to Infrastructure (V2I) communication, the 3D data could be fed into many connected vehicle applications, such as Red-Light Violation Warning and Queue Warning (Q-WARN), to reduce congestion and prevent probable collisions. Though LiDAR is currently a high-maintenance device, as a key perception component of autonomous vehicles, the LiDAR technology evolves rapidly and will soon become a worthy investment thanks to the industrial and academic communities' focus on self-driving technology.

Difficulties arise, however, when applying roadside LiDAR sensors for collecting high-resolution micro traffic data. One of the biggest challenges is the acquisition of a large volume of 3D data that are too sparse and disordered to process, leading to the non-negligible cost of data transmission and processing. Each LiDAR unit produces millions of data points per second, which is a significant barrier to raw data handling and computing. For roadside applications, the best approach for reducing the data workloads is to separate the backgrounds and foregrounds and only keep the targeted objects. Existing roadside LiDAR methods are reference-based, which store an array of background references (e.g., a list of voxels, point clouds, or statistic descriptors) after eliminating moving objects from aggregated frames. The preserved data are used to detect moving objects by comparing new data frames with the background references. These reference-based methods are usually created based on a single indicator, such as mean value, slopes, voxel point density, and maximum value, which is often not appropriate for the multimodal backgrounds. From the theoretical perspective, many well-developed dynamic background models for pixel images are undervalued and were considered not suitable for LiDAR point clouds. As opposed to previous methods, this research attempts to apply the probabilistic-based background modeling method to the roadside LiDAR application in an unsupervised learning manner.

This paper successfully builds a new framework that

P. J. Jin, is associate professor at Civil and Environmental Engineering Department in Rutgers University, Piscataway, NJ 08854 USA (e-mail: peter.j.jin@rutgers.edu)

Yi Ge is PhD candidate at the Civil and Environmental Engineering Department in Rutgers University, Piscataway, NJ 08854 USA (e-mail: yi.ge@rutgers.edu).

implements multimodal background modeling methods for roadside LiDAR object detection. The novel Method transforms 3D point clouds into a structured and compact representation according to elevation and azimuth angular values. The robust and efficient Gaussian Mixture Modeling (GMM) is, for the first time, applied for 3D point clouds without projecting 3D data to a 2D plane. This research expands the knowledge frontier by showing that the conventional image-based background modeling could be effectively applied to the LiDAR detector. The Method resorts to the high-order data structure and provides practical and theoretical foundations to many 3D big data analytics.

The rest of this paper is organized as follows. Firstly, we reviewed the existing literature about LiDAR object detection for both mobile and static LiDAR and pointed out the problems for roadside LiDAR object detection. Then algorithmic details of our methodology are explained and verified through comprehensive experiments and evaluations. At the end of the paper, we highlighted the research contributions and discussed future efforts that can improve the work.

#### II. RELATED WORK

## A. LiDAR Object Detection

Segmenting targets from the surrounding environment is an initial step for LiDAR-based object detection and tracking. Arya [1] developed a 3D-LiDAR Multi-target detection and tracking method in an urban road environment. The detector contains ground removal, segmentation, and bounding box pose estimation. The ground points were identified by checking the elevated points using a slope-based approach. Recent years have already seen many effective deep learning-based LiDAR object detection models developed for self-driving vehicles. Depending on the data representation methods, the deep learning models can be classified into Voxel-based method [2, 3], Point-based method [4], Frustum-based method [5], Pillarbased method [6], and 2D projection-based Method [7~9]. Another way to classify the LiDAR object detection model is based on whether it uses the two-stage region proposal network or one-stage framework [10]. For example, the Yolov3d model builds a 3D object bounding box detection method on the Yolov2 image-based one-shot regression meta-architecture [11]. PointRCNN [12] is a typical region proposal network that first generates a small number of high-quality 3D proposals to segment foreground objects and then refines the 3D proposal in the second state to obtain final detection results.

Recently, the roadside LiDAR began to gain momentum as a new measure of traffic data collection for safety analysis and connected vehicle applications. Compared to the self-driving LiDAR models that are developed for a robot to explore and understand its ever-changing environment, the roadside LiDAR is mainly to detect moving objects in a fixed setting. Given the specific application scenario of roadside LiDAR, most researchers tackle the object detection problem through background filtering. The existing roadside LiDAR background filtering methods are categorized into Point-based, voxelization-based, Projection-based, and Spherical Angular-

based methods [13]. The 3D-density-statistic-filtering (3D-DSF) model [14] considers the points density of LiDAR cloud points in the 3D space. This Method divides the 3D space into discrete cubes and applies frame aggregation, point density statistics, and threshold learning at different ranges to find the background cubes. Image-based method project LiDAR onto the X-o-Y plane and applies the image-based GMM model to detect moving objects, which is at the cost of missing the Z-value of 3D measurements [15]. A variable dimension-based method [16] was developed to store background points instead of storing background voxels by utilizing the static properties of neighbor points.

The searching distance is used to judge whether a point belongs to the neighbor of point A. However, the search distance is affected by not only the manufacturing configuration but also the range of point A. Roadside Lidar was also used for pedestrians and vehicles detection and classification methods at intersections by analyzing the position, velocity, and direction of pedestrians and vehicles [17]. An automatic unsupervised clustering method [18] for LiDAR background in heavy traffic is developed to overcome the LiDAR noises and occlusions under different traffic conditions. The authors divided the 3D space into subspaces and identified the moving objects based on subspace-frame classification, assuming that foreground moving objects cause larger differences from frame to frame. The main drawbacks of voxel-based methods stem from the difficulty of selecting the voxel size that influences the accuracy and computational load. Another study [19] applied a roadside LiDAR detection method through ground points removal and density-based spatial clustering of applications with noise (DBSCAN) and tested its algorithm in both America and China urban environments. In the paper [20], the authors developed a height azimuth background construction method by analyzing the maximum and mean distance of points over the accumulation of data frames with few vehicles or pedestrians. Another Ground plane removal method [21] was applied for vehicle detection and classification system. Their methods include preprocessing, outlier removal, ground plane segmentation, vehicle clustering, key points pair extracting oriented bounding box (OBB), and tracking. A vehicle speed estimation method [22] is explored through background removal, moving point clustering, and vehicle classification. The background removal method is based on the max-distance Method, assuming that the static environment is the furthest point of each laser beam. Table 1 provides a summary of the strengths and limitations of existing roadside LiDAR background subtraction methods.

TABLE I
SUMMARY OF BACKGROUND MODELING BASED ROADSIDE LIDAR OBJECT
DETECTION

BETECHON					
	Data Representat ion	Background/Foregro und Segment Criteria	Strength	Limitation	
Wu et al. (2018); Zhang, Xu and Wu (2020)	Voxel/ 3D Cube	Descriptors of each cube learned from accumulated frames	Accuracy is good for the distance less than 50 meters.	The size of the cube largely influences accuracy and computational cost.	

Zhang, Zheng, Xu and Wang (2019) Zhang, Zheng, Wang, and Fan (2018)	Point Level Cartesian Format  Point Level Cartesian Format	Slope-based Ground Removal and density-based Clustering  Aggregate only background frames and use distance metrics to filter out foreground points	A widely used method for both mobile LiDAR and static LiDAR Easy to Implement	Only can segment ground plane, not able to identify other background objects, such as buildings and trees. We need to accumulate a large number of LiDAR data. Require free flow frames.
Xiao, Vallet, Schindler, and Paparoditi s (2016)	Point Level Cartesian Format	Static Objects have more neighbor points than moving objects over a time window	Temporal Correlation of LiDAR Points	The threshold value of the number of neighboring points is determined based on the researchers' own experience. The density of points varies with range.
Lee and Coifman (2012);So ng et al., (2020)	Vertical and Horizontal Angular	Distance-Based Method at each angular resolution	Spatial Characteristics of Static Points	The fixed distance threshold value does not account for the dynamic background condition
Zhang et al., (2019)	Vertical and Horizontal Map	Compare new data points with the mean and maximum value of constructed background references	Achieved good accuracy at both short-range and long-range	Sensitive to the presence of moving targets for background construction. Not robust under heavy traffic.
Zhao, Xu, Xia, and Liu (2019)	Azimuth Height Table	Height Changes at each beam angular resolution	Good accuracy with the height information for object filtering	Need to select clean background frames for training. Not robust to heavy traffic conditions
Zhang and Jin (2022)	Elevation and Azimuth Matrix	Unsupervised Learning Approach by dynamic clustering and mode decomposition	Using both Intensity and Range information; Parameters are Free and easy to adapt to new conditions	Using a single threshold and hard to capture the dynamic multiple background components

## B. Problems

The deep learning method dominates the LiDAR object detection due to the rapid development of self-driving technology. However, the neural network models are very datahungry. Deep learning models are usually trained on a curated dataset to try to generalize across different scenes, which brings the issue that they can only reliably function under similar scenarios and often don't work for the unseen dataset. As shown in our previous paper [13], the deep neural networks, which were pre-trained on a large-scale public dataset for autonomous driving, are not applicable for roadside LiDAR with a different number of beams. Despite the high potential of the deep learning approach, these models' structures lack transparency, which entails that unsupervised learning approaches are more pragmatic for roadside LiDAR object detection.

The earlier roadside LiDAR background filtering methods that are designed from statistical viewpoints rely on aggregated descriptors to filter out background voxels/points. Existing methods require many samples and manual efforts to correctly maintain the background reference, leading to expensive computation and unsuitable for changing background scenarios. Understanding the unique characteristics of the LiDAR sensor is vitally important before diving into the methodology part. First, the LiDAR data contains non-returnable points when objects are beyond the range limit. LiDAR data has a dual-return mode, meaning only a part of laser pulse comes across an object and reflects from there,

whereas the rest of the pulse keeps travelling till it encounters an object. Second, the stationary background objects in LiDAR data can also tremble due to the rotary pulsed laser beams. LiDAR sensor emits in sequential order at each spin, and the angular values of the same laser beam between two consecutive frames are often drifted, and the offset is larger than azimuth resolution. Last but not the least, LiDAR data is unstructured, meaning that shuffling the 3D points does not change the data. Whereas the image is structured, which will be different after modifying the order of the pixels. Since most background modeling requires structured input, previous studies were not able to apply the pixel-based methods to 3D LiDAR data. The existing challenges and problems call for more adaptable and efficient LiDAR background modeling approach to support roadside LiDAR applications.

#### III. METHODOLOGY

#### A. Data Transformation

Raw LiDAR data contains 3-dimensional measurements and intensity values, as well as GPS information. For the object detection purpose, unstructured LiDAR point clouds need to be transformed as structured representations to enable convolutional or matrix operations. Due to the manufacturing feature, the LiDAR devices don't emit at the fixed angular position for each spin. Therefore, it is not sensible to put LiDAR data points according to their beam ID and sequential firing order. Based on the operational principle of the LiDAR device, each spinning of the LiDAR sensor is considered as a set of spatial slices sampling in the 3D world. Here we apply a hash function to store LiDAR points into stacked spatial slices to transform the point clouds into a high-order structured representation. The functions converting cartesian coordinates into spherical coordinates based on range, elevation, and azimuth angular are described by equation (1) ~ equation (3). **Equations** 

$$x_a = r_a \times \cos(\omega_a) \times \sin(\alpha_a)$$
 (1)

$$y_a = r_a \times cos(\omega_a) \times cos(\alpha_a)$$
 (2)

$$z_a = r_a \times \sin\left(\alpha_a\right) \tag{3}$$

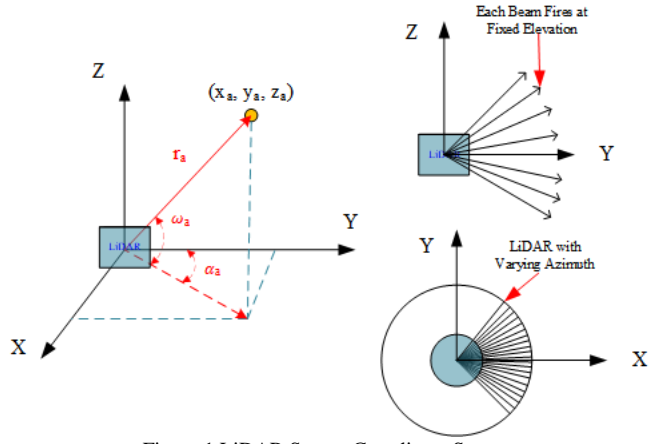


Figure 1 LiDAR Sensor Coordinate System

This study transforms LiDAR data into the tensor structure from the viewpoint of spatial slices at different vertical and horizontal angular. The LiDAR beams are emitting at a fixed vertical angular resolution, and the rotation frequency determines the horizontal angular resolution (See Figure 1). Therefore, we can divide the LiDAR points into each vertical angular and horizontal angular unit. Since the point's vertical angular is associated with fixed beam ID, we only need to identify the proper horizontal angular unit based on rotation frequency. For instance, the horizontal angular resolution for 10 Hz LiDAR is 0.2°, and we will store the data in 360/0.2=1800 different grids. The hash function maps the horizontal angular (α) into an index of the azimuth angular grid.

$$h(\alpha) = mod\left(\left|\frac{\alpha}{Azimuth\ Resolution}\right| + 1,1800\right) \tag{4}$$

Where  $\alpha \in (0, 360]$ .

Instead of dividing the LiDAR model into voxel cells, this operation will arrange the data with structured spherical angular representation according to the beam ID and azimuth value. Eventually, the LiDAR points will be stored in two separate data structures; one contains the range and intensity information, and the other one contains 3D measurements in Cartesian coordinates (Figure 2).

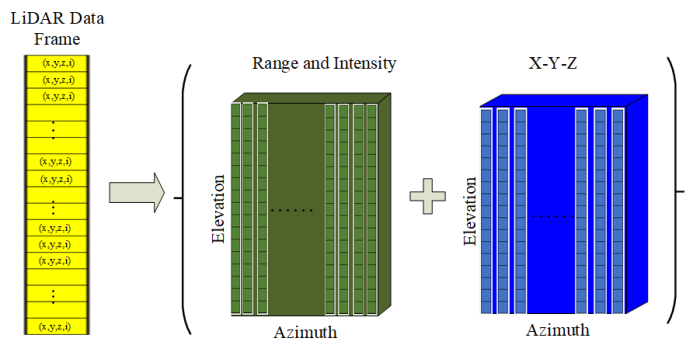


Figure 2 Data Transformation

Processing the LiDAR data in spherical coordinates is consistent with its functioning mechanism. With this transformation, LiDAR points were stored in a Range-Intensity tensor and 3D measurement tensor. Since the elevation is a fixed value for each beam, it is considered a known parameter. The Range-Intensity tensor has the size of Azimuth Grids \* Beams \* 2; For the X-Y-Z tensor, the size is Aimuth Grids \* Beams \* 3. We can draw an analogy between R-G-B channels and grayscale in computer vision with X-Y-Z and Range information. After the data transformation, the unstructured LiDAR point clouds are rearranged into a structured format.

#### B. Multimodal Gaussian Mixture Model

In this section, we will fit the X-Y-Z and range-intensity tensor to Gaussian Mixture Models. The two tensors can be used separately or combined for better detection. The GMM models  $[24 \sim 27]$  have been developed for decades and are still an active research topic, which is implemented with a lot of

skills and experience for satisfiable real-time performance. Fortunately, compared to the camera sensor, the LiDAR sensor does not experience moving shadows, camouflage (foregrounds have similar colors to the background), sudden illumination changes, and challenges like that. The GMM method is an excellent method to handle the dynamic LiDAR data backgrounds. The probabilistic GMM model that learns the background subcomponents is described as follows.

A recent data set of measurements  $M_T = \{m_1, m_2, ..., m_T\}$  over a period T is captured by a mixture of K Gaussian distributions. For each elevation-azimuth unit at time t is estimated by:

$$P(m_t) = \sum_{k=1}^{K} \omega_{k,t} * \eta(m_t, \mu_{k,t}, \Sigma_{k,t})$$
 (5)

Where K is the number of Gaussian Distributions, which determined the multimodality of background, conventionally as 3, 5, or 7.  $\omega_{k,t}$  is the weight associated to the  $k^{th}$  Gaussian at the time t with mean and covariance matrix  $\mu_{k,t}$ ,  $\Sigma_{k,t}$ .  $\eta(\cdot)$  is the Gaussian Probability function given by:

$$\eta(m_t, \mu, \Sigma) = \frac{1}{(2\pi)^{\frac{n}{2}} |\Sigma|^{\frac{1}{2}}} \exp{-\frac{1}{2}(m_t - \mu)^T \Sigma^{-1}(m_t - \mu)}$$
(6)

Where n is the dimension of measurement, in our model, we can use n = 3 for the X-Y-Z tensor and n = 2 range-intensity tensor

In the LiDAR measurements, X-Y-Z 3D measurements are orthogonal and assumed to have the same variance. The covariance matrix is then simplified by:

$$\Sigma_{\nu} = \delta_{\nu}^2 I \tag{7}$$

With this property, a costly matrix inversion is avoided. The parameters including the weight  $\omega_{k,t}$  the mean  $\mu_{k,t}$  and the covariance matrix  $\Sigma_k$  could be initialized using Expectation Maximization (EM) algorithm to maximize the likelihood of the input data. For computational reasons, online clustering approach K-means algorithm is used to replace EM algorithm for real-time application. Every new distance measurement  $m_t$ is checked against the existing K Gaussian distributions, until a match is found, which is defined within 2.5 standard deviations of a distribution. If Gaussian distribution is background component, then the new point is classified as background, otherwise it will be classified as foreground. If no match was found with all K Gaussians, the point is classified as foreground. After iterating all points, a foreground mask is obtained to make foreground detection. This foreground mask generation method has been validated as an effective method on existing video based GMM model.

Fomultimodal GMM models, the ratio  $\omega/\delta$  is used to order the K Gaussians. The background points correspond to a higher weight with a weak variance than moving objects because the background points are practically constant. The first B Gaussian distributions larger than certain threshold T are retained for background components.

$$B = \arg\min_{b} \sum_{k=1}^{b} \omega_k > T \tag{8}$$

As an online learning procedure, the weight parameters are updated as follows:

$$\omega_{k,t} = \begin{cases} (1-\alpha)\omega_{k,t-1} + \alpha, & \text{for matched Gaussian Components} \\ (1-\alpha)\omega_{k,t-1}, & \text{for unmatched Gaussian Componenets} \end{cases}$$
(9)

The mean and variance for the unmatched components remain unchanged, and for the matched component, they are updated as given below:

$$\mu_{k,t} = (1 - \rho)\mu_{k,t-1} + \rho \cdot m_t$$

$$\sigma_{k,t}^2 = (1 - \rho)\sigma_{k,t-1}^2 + \rho (m_t - \mu_{k,t-1})^T \cdot (m_t - \mu_{k,t-1})$$
(11)

where  $\rho = \alpha \cdot \eta(X_t, \mu_{k,t}, \Sigma_{k,t})$ .

For another case where a point does not match with any of the K Gaussians, the distribution with the least probability is updated with the new parameters  $(\omega_{L,t}, \mu_{L,t}, \sigma_{L,t}^2)$ .

$$\mu_{Lt} = m_t \tag{12}$$

$$\omega_{Lt} = Initial \ low \ prior \ weight$$
 (13)

$$\mu_{L,t} = m_t$$
 (12)  
 $\omega_{L,t} = Initial \ low \ prior \ weight$  (13)  
 $\sigma_{L,t}^2 = Initial \ High \ Variance$  (14)

The LiDAR data generate spatial slices of its surrounding environment with high frequency. Due to the sequentially firing mechanism, the pulsed light might hit different parts of the same background components, resulting in multimodal distributions. Thus, modeling LiDAR backgrounds as a mixture of Gaussian distributions makes rational sense. Furthermore, the proposed Method inherits many of the theoretical and computational benefits of GMMs, making it practical for 3D big data processing.

## C. The Realtime Roadside LiDAR Detection Framework

The entire workflow is broken down into the following steps (see Figure 3). The first step is to transform LiDAR packet data into a tensor format using the hash function. The second step is to determine the detection zone. A large amount of the backgrounds are distant buildings. This can be done with Geofencing to filter out nondrivable or walkable space based on GPS location. Next, the GMM background modeling will be applied to create foreground masks using the combination of range-intensity and X-Y-Z measurements. The local Outlier Factor (LOF) algorithm is used to remove noisy points that are left out by background modeling steps. After finishing that, a density clustering-based bounding box estimator was used to obtain detections from the segmented objects. Each detected object was encoded into a state space with 3-dimensional coordinates, angles, and speeds. The detected object is classified into different road user groups, including pedestrians, passenger cars, trucks, and large freight vehicles. The object classification is based on detection bounding box 3D measurements, length/height ratio, and traveling speeds. Then

a joint probabilistic data association (JPDA) and interacting multiple model (IMM) filter are applied to track each object over continuous frames.

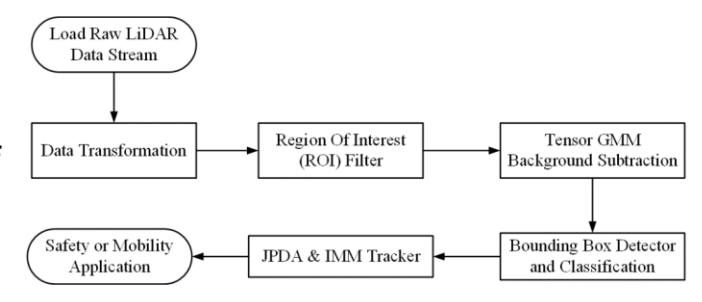


Figure 3 Real-Time LiDAR Object Detection, Classification, and Tracking with GMM Model

#### IV. EXPERIMENTAL SETUP

#### A. Testing Sites

Two testing sites are selected. Both are installed with 2K cameras and Alpha Prime LiDAR Sensors with communication and power cables. The first site is at the intersection between Albany Street and George Street in downtown New Brunswick, affinity to many restaurants, banks, and university campus; The second site is at the French street and Joyce Kilmer Ave, which is close to the Robert Wood Johnson hospital with the largest number of employees in this area. The construction plan is a part of the new 2.4-mile Data City Smart Mobility Testing Ground by Rutgers University's Center for Advanced Infrastructure and Transportation (CAIT) to establish a living laboratory for connected and automated vehicle technologies in New Jersey. Eventually, multiple intersections from the testing corridors will be equipped with high-resolution roadside sensors and edge computing devices to enable smart mobility applications. LiDAR sensors play a critical role in addressing intersection queuing, identifying near-miss events, and empowering digital-twin technology for traffic management. The selected intersection layouts and sensors' locations are shown in Figure 4.



Testing Site 2: French St @ Joyce Kilmer Ave



Figure 4 Testing Sites at New Brunswick Smart Mobility Testing Ground

The first testing site is from Albany Street @ George Street, located in downtown New Brunswick, representing a busy urban arterial with signal control. For the first testing site, the data is collected during morning peak hours on Dec 15, 2021, under heavy traffic conditions. The data from the second testing site, French St @ Joyce Kilmer Ave, were collected on Jan 20, 2022, a snowy day, to investigate how the weather condition could impact LiDAR performance. We use the 2.7k cameras mounted on the same traffic pole to generate directional counts and compare them against our LiDAR GMM background subtraction methods to evaluate the performance quantitively.

## B. Benchmark Computer Vision Algorithms

Computer Vision vehicle detection and tracking model is built on instance segmentation network Mask R-CNN [28] that has the backbone of ResNeXt-101 feature pyramid network [29]. Five object classes of interest, including car, truck, person, bus, and bike, are used according to the Microsoft COCO dataset [30]. A Weighted Inter-class Non-maximum Suppression (WINS) is applied to remove false interclass detections, as small trucks could result in car and truck double detections. In this case, we prefer to remove the car detection. The online association algorithm is employed to assign detections from new frames to existing tracklets, considering both feature similarity and spatial constraints. The outputs of computer vision algorithms are used to evaluate the LiDAR detection results at the trajectory level. The detected objects and tracked trajectory points from the high accuracy computer vision algorithms are shown in Figure 5.





Figure 5 Computer Vision Benchmark Detection and Tracking

#### V. RESULTS ANALYSIS

In this section, we will comprehensively analyze the efficacy of proposed methodology from point level, object level and path level.

#### A. Point Level Evaluation

The point level results are the fundamental step for foreground segmentation. This evaluation part aims to quantify the efficiency of GMM background subtraction for each LiDAR point. To get ground truth data, we manually removed background objects from randomly selected LiDAR data frames. Each point from LiDAR detection results and ground truth data can be classified as a true positive, true negative, false positive, or false negative. Four performance metrics were used, including Accuracy, Precision, Recall, and F1 score, which were defined in the following equations. Two state-of-the-art roadside LiDAR background modeling methods were implemented as baseline models against the same ground-truth dataset.

$$Accuracy = \frac{TP + TN}{TP + TN + FP + FN} \tag{15}$$

$$Precision = \frac{TP}{TP + FP} \tag{16}$$

$$Recall = \frac{TP}{TP + FN} \tag{17}$$

$$F1 Score = 2 * \frac{Precision * Recall}{Recall + Precision}$$
 (18)

The two baseline models are chosen because they are very like our Method, that is built on spherical coordinates. The first baseline model is called Coarse-Fine Triangle Algorithm (CFTA), which applies histogram triangle thresholding to automatically find the dividing value between foreground targets and background objects. The second baseline model is a two-step approach to establish the background range for each elevation-azimuth value by using the mean and max values calculated from a large number of frames. As shown in the table below, our GMM model outperformed the baseline methods by all metrics in two scenarios. The accuracies of all models are very high because the background and foreground point clouds are highly imbalanced. According to our 128 beam LiDAR dataset, the background objects account for 95% of the total point clouds (Figure 6). The high accuracy scores suggest that most background components can be correctly removed using all methods.

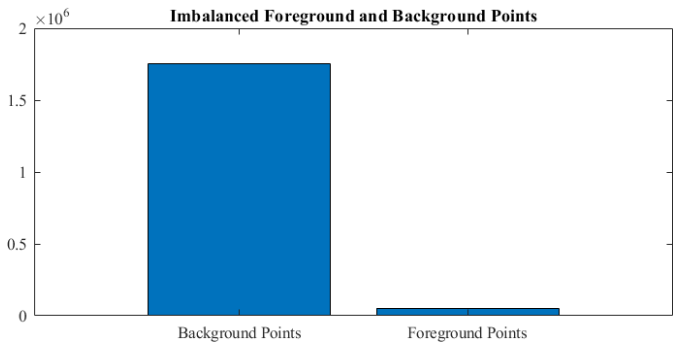


Figure 6 Imbalance Backgrounds and Foregrounds in 128 Beam Roadside
LiDAR Point Clouds

Due to the impact of snow, the foreground detection results on Site-2 show lower Precisions than on Site-1. The snowstorm exerts the greatest influence on the Mean-Max model that uses basic mean and maximum values for background construction. While the GMM method demonstrates the best robustness under snowy weather among all three methods, evidenced by

the highest Precision score on the Site-2 intersection. Overall, our multimodal GMM algorithm has the best performance on all four categories (See TABLE II).

In Figure 7, the foreground segmentation results are presented. The scatted points in the air are falling snow. All three models are inevitably impacted by the phantom LiDAR points under the challenging weather. Among all comparable methods, the GMM model is the most efficient, with the cleanest background points.

TABLE II
POINT LEVEL EVALUATION RESULTS

	Testing Site 1: George @ Albany			Testing	Site 2: Frenc	h @ Joyce l	Kilmer	
	Accuracy	Precision	Recall	F1 Score	Accuracy	Precision	Recall	F1 Score
GMM	98.8%	96.1%	93.6%	94.8%	99.5%	84.9%	95.2%	89.8%
CFTA	98.0%	90.2%	92.3%	91.2%	98.6%	64.1%	79.9%	71.1%
Mean- Max	90.9%	55.0%	85.1%	66.8%	94.2%	22.8%	72.9%	34.7%

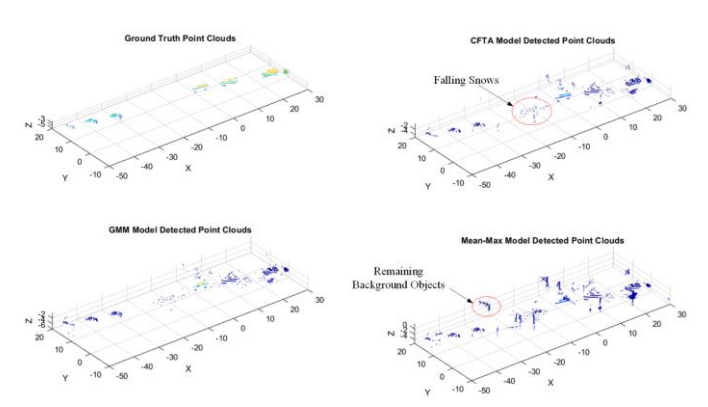


Figure 7 Point Level Foreground Segmentation Evaluation

## B. Object Level Evaluation

The purpose of the object-level evaluation is to evaluate how the occlusion and bad weather could impact object recognition based on the segmented foreground points. For object-level assessment, we conducted the 3D bounding box assessment from selected data frames at 300 intervals. We went through the extracted frames with 3D object bounding box detections to judge whether each bounding box was correct or if any missed detection happened. The validation of object-level detection is summarized with the number of True Positives, False Negatives, and False Positives, which are then used for calculating Precision, Recall, and F1 Score.

For Site-1, the occlusion issues are significant during the red signal phase due to front vehicles in the queue often blocking the following vehicles, resulting in fewer LiDAR points for the detector to create a bounding box. Therefore, the Recall score at Site-1 is low. From all the selected frames, very few false positives were found in Site-1, showing the GMM model can efficiently remove background points. For Site-2 intersection, the vehicle volume is lower, causing fewer occlusions. Due to the impact of the snowstorm, the precision score on Site-2 is lower than the Site-1 intersection. The density-based detector

falsely generated a bounding box for the falling snows when phantom LiDAR points are greater than the detector's threshold.

TABLE III
OBJECT LEVEL EVALUATION RESULTS

	Testing Site 1: Albany @ George	Testing Site 2: French @ Joyce Kilmer
Precision	99.03%	97.41%
Recall	78.21%	90.40%
F1 Score	87.39%	93.78%

Figure 8 displays the main occlusions at the signalized intersection caused by the queuing vehicles during the red light phase. Vehicles on outer lanes are often blocked by vehicles on the closed lanes. However, after the signal turns green, these blocked vehicles could be detected again as the gaps between vehicles get large enough.

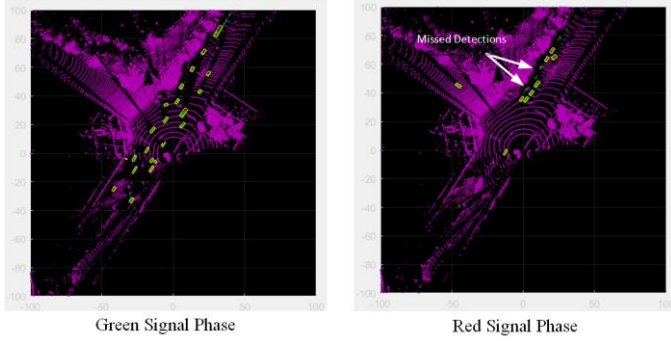


Figure 8 Object Level Detection Results Evaluation

#### C. Path Level Evaluation

The previous point level and object level evaluations are performed on static LiDAR frames, whereas the path level evaluation is used to examine the tracking module performance with bounding box detections for continuous LiDAR frames. In Figure 9, the segmented foreground using GMM and bounding box detection results are presented side-by-side. The red boxes are bounding box measurements in 3D dimensions with orientation angle. The green box is tracked object based on historical records. In our settings, if the bounding box is observed consecutively for six frames, we will change that object's status from candidates to confirmed objects. The tracked object is missing nine frames in the past ten frames, and then the algorithm will delete the objects from the tracking records. The algorithm can efficiently overcome the occlusion problem when tracked vehicles are temporarily obstructed by vehicles in the adjacent lane.

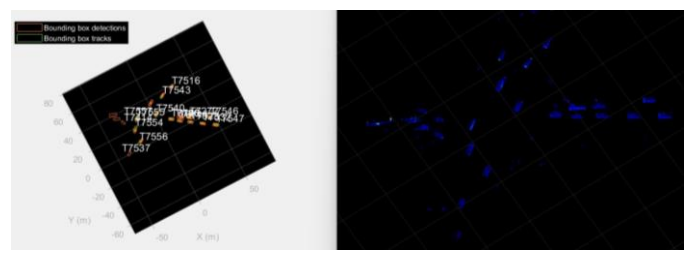


Figure 9 Bounding Box Detection and Tracking on Segmented Moving Vehicles

For the selected intersection, each camera mainly faces one approach. We choose the approach that has the highest traffic volume and compares the inbound and outbound traffic volume within 15-min to examine the path level object detection results. The computer vision model is named as Zero-shot VehIcle Route Understanding System (Zero-VIRUS) [31], which is a top-3 winner from CVPR AI City Challenge for traffic camera movement counts. The parameters were mostly maintained the same in this experiment, except that the original version detects three classes while our implementations have five classes. The camera views from two testing sites are shown in Figure 5. Testing results show that our tracking model produces good accuracy under both congested conditions and challenging weather conditions. All movement counting accuracies are above 92%. The extracted trajectories from two locations were plotted in Figure 10, containing both the vehicles and pedestrians. The trajectory data can be used for analyzing pedestrian safety issues to near-miss events at intersections.

TABLE IV
PATH LEVEL EVALUATION RESULTS

	Testing Site 1: Albany @ George		Testing Site 2: French @ Joyce Kilmer	
	inbound	outbound	inbound	outbound
Video Count	211	221	86	92
LiDAR Count	223	204	82	88
Accuracy	Accuracy 94.31% 92.31%		95.35%	95.65%

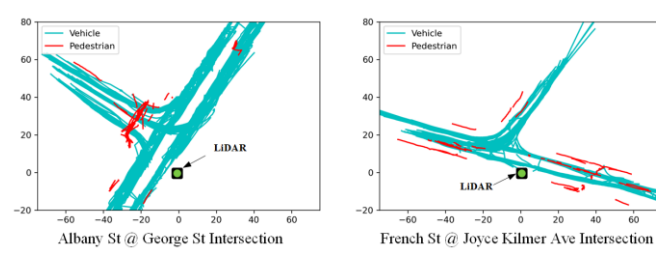


Figure 10 Vehicle and Pedestrian Trajectory Using Proposed Method

## VI. DISCUSSION

Applying GMM for roadside LiDAR object detection can significantly improve the efficiency of point cloud processing. In Figure 11, we use the GMM to build the background model as static data and only update the foreground vehicle LiDAR points. That's the reason why it doesn't contain shadows as the

original LiDAR point clouds. An animated version can be found on our project repository [32].

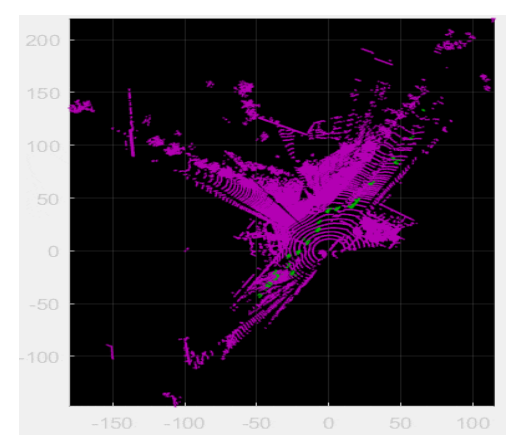


Figure 11 Segmented Moving Object Overlayed on Pretrained Background

For roadside LiDAR, the object detection task only pertains to a small amount of data in a fixed environment. The background modeling can significantly improve the data chain efficiency by only transitioning a tiny portion of the foreground LiDAR point clouds. In our testing experiment, 31.7 GB of raw point cloud data were compressed into 760 MB foregrounds and a background reference, which reduced around 95% redundancy in roadside LiDAR data.

The outcome of this research will help to integrate the infrastructure-based LiDAR into connected intersection applications. In Figure 12, the lane-by-lane queue length could be easily acquired using the object detection method. The LiDAR measurements can be turned into input for adaptive traffic signal control and enable traffic managers to monitor systems in real-time. Besides mobility applications, the roadside LiDAR sensor can also be used for safety-critical applications. For instance, LiDAR detection could identify near-miss situations at intersections and generate safety performances for signalized intersections. As opposed to the conventional detector (e.g., Loop Detector, Radar) that are installed at fixed locations and only produce spot information, the LiDAR sensor generates much more extensive coverage as an ideal digital solution for smart infrastructure.

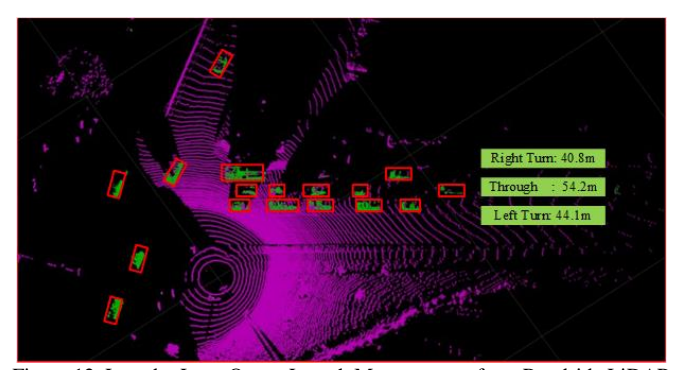


Figure 12 Lane by Lane Queue Length Measurement from Roadside LiDAR After Background Subtraction

In terms of implementation, the GMM model offers two modes. One is the static background mode, and the other is the dynamic background mode. The static background mode has a minimum learning rate that updates the background in an extremely slow fashion; The dynamic background with a larger learning rate is more adaptive that can adjust its background parameters in real-time. The shortcoming of static background mode is that the background does not reflect the exact current environment, as the static background is pre-trained beforehand. The dynamic background mode has the issue of sleeping objects when vehicles wait before red light for a long duration, and the dynamic GMM model will consider those vehicles as stationary backgrounds.

#### VII. CONCLUSION

Traditional probabilistic-based and pattern recognition techniques have encompassed many classic algorithms for video-based background modeling. However, these very mature techniques haven't been successfully utilized for roadside LiDAR background modeling. The main reason is that LiDAR data is inherently unstructured and sparse in space, whereas the images are rather structured. This research appears to be the first study that successfully adopted the classical GMM model for 3D LiDAR object detection. Specifically, the probabilistic density function is used at every elevation-azimuth unit to construct the density function of X-Y-Z measurement for background representation. This Method allows for stable and rapid adaptation to a dynamic environment for an assortment of surveillance applications.

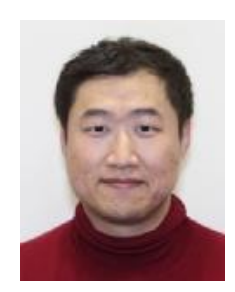
Compared to neural-network-based approaches, the GMM methods, which process the data in sequential steps and do not require multi-processing supported by GPU parallelism capability, are suitable for budget-constrained agencies. Different from existing roadside LiDAR background modeling methods that rely on hand-crafted engineering to filter out background points, this solution is a plug-and-play unsupervised learning approach with a strong theoretical foundation. The algorithm of the GMM LiDAR model can be effortlessly generalized to various scenarios for high-dimensional data processing. The foreground/background segmentation method could be used to build future-oriented cyber-physical systems in smart cities.

#### REFERENCES

- Arya Senna Abdul Rachman, A. (2017). 3D-LIDAR multi object tracking for autonomous driving: multi-target detection and tracking under urban road uncertainties.
- [2] Engelcke, M., Rao, D., Wang, D. Z., Tong, C. H., & Posner, I. (2017, May). Vote3deep: Fast object detection in 3d point clouds using efficient convolutional neural networks. In 2017 IEEE International Conference on Robotics and Automation (ICRA) (pp. 1355-1361). IEEE.
- [3] Zhou, Y., Tuzel, O.: Voxelnet: End-to-end learning for point cloud based 3d object detection. arXiv preprint arXiv:1711.06396 (2017)
- [4] Qi, C. R., Su, H., Mo, K., & Guibas, L. J. (2017). Pointnet: Deep learning on point sets for 3d classification and segmentation. In *Proceedings of the IEEE conference on computer vision and pattern recognition* (pp. 652-660).
- [5] Gong, Z., Lin, H., Zhang, D., Luo, Z., Zelek, J., Chen, Y., ... & Li, J. (2020). A Frustum-based probabilistic framework for 3D object detection by fusion of LiDAR and camera data. *ISPRS Journal of Photogrammetry* and Remote Sensing, 159, 90-100.

- [6] Lang, A. H., Vora, S., Caesar, H., Zhou, L., Yang, J., & Beijbom, O. (2019). Pointpillars: Fast encoders for object detection from point clouds. In *Proceedings of the IEEE/CVF Conference on Computer Vision and Pattern Recognition* (pp. 12697-12705).
- [7] Li, B., Zhang, T., & Xia, T. (2016). Vehicle detection from 3d lidar using fully convolutional network. arXiv preprint arXiv:1608.07916.
- [8] Chen, X., Ma, H., Wan, J., Li, B., & Xia, T. (2017). Multi-view 3d object detection network for autonomous driving. In *Proceedings of the IEEE* conference on Computer Vision and Pattern Recognition (pp. 1907-1915).
- [9] Asvadi, A., Garrote, L., Premebida, C., Peixoto, P., & Nunes, U. J. (2017, October). DepthCN: Vehicle detection using 3D-LIDAR and ConvNet. In 2017 IEEE 20th International Conference on Intelligent Transportation Systems (ITSC) (pp. 1-6). IEEE.
- [10] Fernandes, D., Silva, A., Névoa, R., Simoes, C., Gonzalez, D., Guevara, M., ... & Melo-Pinto, P. (2021). Point-cloud based 3D object detection and classification methods for self-driving applications: A survey and taxonomy. *Information Fusion*, 68, 161-191.
- [11] Ali, W., Abdelkarim, S., Zidan, M., Zahran, M., & El Sallab, A. (2018). Yolo3d: End-to-end real-time 3d oriented object bounding box detection from lidar point cloud. In *Proceedings of the European Conference on Computer Vision (ECCV) Workshops* (pp. 0-0).
- [12] Shi, S., Wang, X., & Li, H. (2019). Pointrenn: 3d object proposal generation and detection from point cloud. In *Proceedings of the IEEE/CVF conference on computer vision and pattern recognition* (pp. 770-779).
- [13] Zhang, T., & Jin, P. J. (2022). Roadside Lidar Vehicle Detection and Tracking Using Range And Intensity Background Subtraction. arXiv preprint arXiv:2201.04756.
- [14] Wu, J., Xu, H., Sun, Y., Zheng, J., & Yue, R. (2018). Automatic background filtering method for roadside LiDAR data. *Transportation Research Record*, 2672(45), 106-114.
- [15] J. Zhang, W. Xiao, B. Coifman and J. P. Mills, "Image-based vehicle tracking from roadside LiDAR data", Int. Arch. Photogramm. Remote Sens. Spatial Inf. Sci., vol. 42, pp. 1177-1183, Jun. 2019.
- [16] Wu, J., Lv, C., Pi, R., Ma, Z., Zhang, H., Sun, R., ... & Wang, K. (2021). A Variable Dimension-Based Method for Roadside LiDAR Background Filtering. *IEEE Sensors Journal*, 22(1), 832-841.
- [17] Zhao J, Xu H, Liu H, Wu J, Zheng Y, Wu D. Detection and tracking of pedestrians and vehicles using roadside LiDAR sensors. Transportation research part C: emerging technologies. 2019 Mar 1;100:68-87.
- [18] Zhang, Y., Xu, H., & Wu, J. (2020). An automatic background filtering method for detection of road users in heavy traffics using roadside 3-D LiDAR sensors with noises. IEEE Sensors Journal, 20(12), 6596-6604.
- [19] Zhang Z, Zheng J, Xu H, Wang X. Vehicle Detection and Tracking in Complex Traffic Circumstances with Roadside LiDAR. Transportation Research Record. 2019;2673(9):62-71. doi:10.1177/0361198119844457.
- [20] Z. Zhang, J. Zheng, H. Xu, X. Wang, X. Fan and R. Chen, "Automatic Background Construction and Object Detection Based on Roadside LiDAR," in *IEEE Transactions on Intelligent Transportation Systems*, vol. 21, no. 10, pp. 4086-4097, Oct. 2020, doi: 10.1109/TITS.2019.2936498.
- [21] Sun, Y., Xu, H., Wu, J., Zheng, J., & Dietrich, K. M. (2018). 3-D Data Processing to Extract Vehicle Trajectories from Roadside LiDAR Data. *Transportation Research Record*, 2672(45), 14–22. https://doi.org/10.1177/0361198118775839
- [22] Zhang, J., Xiao, W., Coifman, B., & Mills, J. P. (2020). Vehicle tracking and speed estimation from roadside lidar. IEEE Journal of Selected Topics in Applied Earth Observations and Remote Sensing, 13, 5597-5608.
- [23] Zhao J, Xu H, Xia X, Liu H. Azimuth-Height background filtering method for roadside LiDAR data. In2019 IEEE Intelligent Transportation Systems Conference (ITSC) 2019 Oct 27 (pp. 2421-2426). IEEE.
- [24] KaewTraKulPong, P., & Bowden, R. (2002). An improved adaptive background mixture model for real-time tracking with shadow detection. In *Video-based surveillance systems* (pp. 135-144). Springer, Boston, MA.
- [25] Stauffer, C., & Grimson, W. E. L. (1999, June). Adaptive background mixture models for real-time tracking. In *Proceedings. 1999 IEEE* computer society conference on computer vision and pattern recognition (Cat. No PR00149) (Vol. 2, pp. 246-252). IEEE.
- [26] Goyal K, Singhai J. Review of background subtraction methods using Gaussian mixture model for video surveillance systems. Artificial Intelligence Review. 2018 Aug;50(2):241-59.

- [27] Bouwmans, T., El Baf, F., & Vachon, B. (2008). Background modeling using mixture of gaussians for foreground detection-a survey. *Recent* patents on computer science, 1(3), 219-237.
- [28] He, K., Gkioxari, G., Dollár, P., & Girshick, R. (2017). Mask r-cnn. In Proceedings of the IEEE international conference on computer vision (pp. 2961-2969).
- [29] Lin, T. Y., Dollár, P., Girshick, R., He, K., Hariharan, B., & Belongie, S. (2017). Feature pyramid networks for object detection. In *Proceedings of the IEEE conference on computer vision and pattern recognition* (pp. 2117-2125).
- [30] Lin, T. Y., Maire, M., Belongie, S., Hays, J., Perona, P., Ramanan, D., ... & Zitnick, C. L. (2014, September). Microsoft coco: Common objects in context. In *European conference on computer vision* (pp. 740-755). Springer, Cham.
- [31] Yu, L., Feng, Q., Qian, Y., Liu, W., & Hauptmann, A. G. (2020). Zerovirus: Zero-shot vehicle route understanding system for intelligent transportation. In *Proceedings of the IEEE/CVF Conference on Computer Vision and Pattern Recognition Workshops* (pp. 594-595).
- [32] https://github.com/TeRyZh/Gaussian-Mixture-Model-for-Roadside-LiDAR-Object-Detection-and-Tracking



**Tianya Zhang** received PhD degree in Transportation Engineering from the Department of Civil and Environmental Engineering at Rutgers University. He earned master's degrees in Transportation Engineering from Texas A&M University, and Computer Science from University of Pennsylvania.

He is an incoming Postdoc at the CIRCLES Consortium, working on

collaborative driving. He has been involved in several ITS projects related to Automated Traffic Signal Performance Measures (ATSPMs) and Smart Mobility Testing Ground. His research using computer vision and LiDAR for vehicle trajectory detection has been published in Transportation Research Part C and Transportation Research Record.



Peter J. Jin was an Associate Professor at Department of Civil and Environmental Engineering (CEE) at Rutgers, The State University of New Jersey. He received the BS degree in Automation at Tsinghua University, China. He received his MS and Ph.D. degrees in civil engineering from University of Wisconsin-Madison in 2007 and 2009 respectively. He worked at Center for Transportation Research, at the University of Texas at Austin as a postdoctoral fellow and research associate. He has more than 45 peer-

reviewed journal publications and more than 70 conference papers. His research interests include transportation big data analytics, intelligent transportation systems, connected and automated vehicles (CAVs), and unmanned aerial vehicles (UAVs). He holds two patents in both UAVs and CAVs.



Yi Ge received MS degree in Transportation Engineering from the Department of Civil and Environmental Engineering at Rutgers University in 2020 and continued to pursuing PhD degree in Transportation Engineering since then. He won the ITSNJ 2020 Outstanding Graduate Student Award and ITSNJ 2021 Future of ITSNJ Award.